Archives of Materials Science and Engineering

Volume 42
Issue 2
April 2010
Pages 85-92

International Scientific Journal
published monthly by the
World Academy of Materials
and Manufacturing Engineering

Corrosion of evaporator tubes in low emission steam boilers

S. Topolska [a,*], J. Łabanowski [b]

[a] Institute of Engineering Materials and Biomaterials,
Silesian University of Technology, ul. Konarskiego 18a, 44-100 Gliwice, Poland
[b] Faculty of Mechanical Engineering, Gdansk University of Technology,
ul. Narutowicza 11/12, 80-233 Gdańsk, Poland
* Corresponding author: E-mail address: santina.topolska@polsl.pl

Received 22.02.2010; published in revised form 01.04.2010

ABSTRACT

Purpose: of this paper is to reveal the mechanisms of corrosion processes of outer surfaces of low-emission steam boiler evaporator tubes. Examinations were performed to find the reasons of different corrosion susceptibility of tubes situated at combustion chamber on various levels.

Design/methodology/approach: Examinations were conducted on several segments of Ø 57 x 5.0 mm evaporator tubes made of 16M (16Mo3) steel grade. Segments were taken from level of 10 meters and 18 meters from the chamber bottom of low-emission coal fired steam boiler after two years operation. Microstructure degradation of base material was estimated. Metallographic evaluation of scale morphology, its micro sites chemical composition analysis and distribution of elements on cross sections have been performed.

Findings: Eexaminations of evaporator tubes indicated that reduction of wall thickness was considerable at the segments taken from level of 10 m, when at level of 18 m this reduction was small. The morphology of scales consisted of external layer which was porous and weakly connected to the tube surface, and internal layer, which was dense and adherent to the base metal. In these two layers the bands reach in sulfur were detected. The sulfide corrosion seems to be the main degradation mechanism of the tube surface at the level of 10 m.

Research limitations/implications: Corrosion of the water wall tubes in low-emission steam boilers is a result of reaction of steel tube surface with the aggressive substoichiometric environment contains sulfur. The chemical composition of flue gases changes along the water wall. The exact compound of flue gases has not been determined in this study.

Practical implications: Prevention of water wall tubes corrosion can be achieved by changing in operation conditions or replacement of tube materials. The first mentioned action is limited to accurate burner's adjustment or introduces a flow of additional air along the walls and create air curtain between reducing environment and tubes surface. These efforts often are insufficient. The replacement of more corrosion resistant material on Cr rich steel or Cr-Ni steel is possible but other problems appear connected with high costs of installation and low heat transfer coefficients of such materials. Knowing the mechanisms of corrosion allows adjusting combustion process at low emission steam boilers.

Originality/value: Information available in literature does not clearly indicate what mechanism of corrosion is dominant at different parts of combustion chamber. The current study shows which corrosion mechanisms are the most dangerous for evaporator tubes.

Keywords: Corrosion; Low-emission steam boiler; Evaporator tubes; Sulfide corrosion

Reference to this paper should be given in the following way:

S. Topolska, J. Łabanowski, Corrosion of evaporator tubes in low emission steam boilers, Archives of Materials Science and Engineering 42/2 (2010) 85-92.

PROPERTIES

1. Introduction

Corrosion of water walls is the serious problem in low-emission coal fired boilers operation. Modification of combustion process was developed for limitation nitride oxides (NO_x) emission. Ashes and solid particles from the flue gases are eliminated on electro filters but reduction of nitride oxides can be achieved by limitation of air excess at the burners exhaust area at furnace chamber. Application of the low-emission combustion process results in increase corrosion of furnace walls. The major causes of tube corrosion are: the reducing (substoichiometric) gas environment causing sulfide corrosion and/or molten salt attack [1-5].

Corrosion from the firing of coal is related to specific impurities in the fuel like sulfur, sodium, potassium, chlorine, and incombustible mineral matter which produces ash during combustion. Fly ash can deposit on cooler components like furnace walls. This provides a mechanism for the accumulation of deposits on cooled surfaces.

Prevention of water wall tubes corrosion can be achieved by changing in operation procedures and replacement of tube materials [6]. The first mentioned action is limited to accurate burners adjustment or introduce a flow of additional air along the walls and create air curtain between reducing environment and tubes surface. These efforts often are insufficient. The replacement of more corrosion resistant material on Cr rich steel or Cr-Ni steel is possible but other problems appear connected with high costs of installation and low heat transfer coefficients of such materials [7, 8].

The objective of this study is to show the main corrosion mechanisms of water walls and compare the corrosion processes occur on different levels of combustion chamber at low emission boiler.

2. Experimental

Examinations were conducted on four segments of ∅ 57 x 5.0 mm evaporator tubes made of 16M (16Mo3) steel grade. Segments were taken from two tubes at levels 10 and 18 meters from the chamber bottom. The highest row of burners was situated on the level 14 meters. Tubes were in operation for two years.

Tubes wall thicknesses were measured on the cross sections at the places indicated in Fig. 1. The results are collected in Table 1. The reduction in wall thickness was not uniform on tube's perimeter. The front side of the tube facing the combustion radiant heat suffered the worst metal wastage and reaches 58% of its nominal value. Reductions in wall thickness from insulation side of tubes were not observed. The highest reduction in wall thickness was detected at points 1 and 3 from the fire side of the tube. Thickness reduction was considerable on the segments taken from the level of 10 m, when at level 18 m this reduction was small.

The view of cross section of the tube surface is shown in Fig.2. The deposits on the tube's surfaces differ in the thickness from 100 to 300 μm. Scale consists of two layers, external, which is porous and weakly connected with the tube surface, and internal, which is dense and adherent to the base metal.

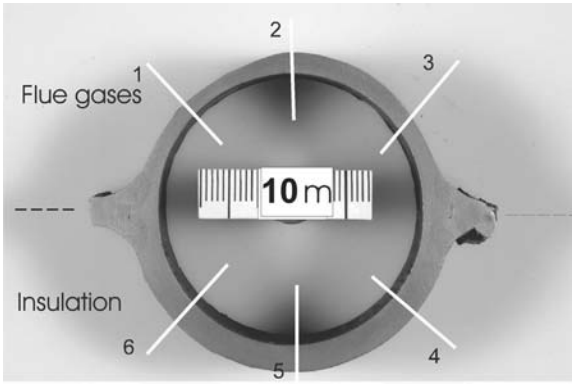

Fig. 1. Cross section of ∅ 57 x 5.0 mm evaporator tube (level of 10 m)

Table 1.
Tubes wall thickness

Tube/ height from bottom, m	Wall thickness, mm			
	Insulation side (mean value)	Flue gases side		
point→	4, 5, 6	1	2	3
42D/10	5.0	2.9	3.5	3.0
42G/18	5.0	3.2	3.8	3.3
51D/10	5.0	2.9	3.1	2.9
51G/18	5.0	3.3	3.5	3.2

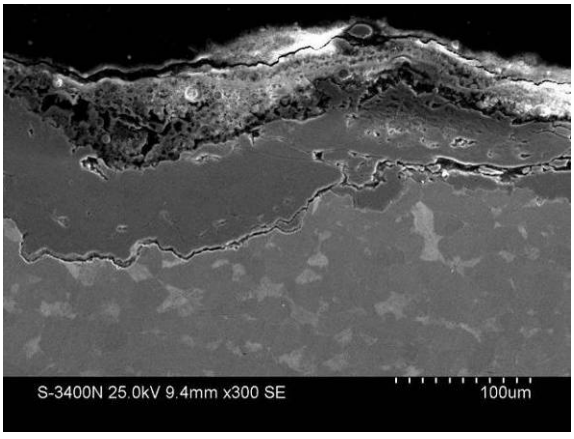

Fig. 2. Cross section of ∅ 57 x 5.0 mm evaporator tube after two years exploitation. Deposits on the fireside of the tube

Preliminary investigations of tubes were conducted for evaluation of base material condition after two years exploitation. The main aim of tests was to indicate the influence of high temperature operation on microstructure changes and mechanical properties of 16M steel (comp.: [9]). The outer metal skin temperature of the furnace walls should be kept at temperatures below 450°C, but substoichiometric combustion and thick scales

on the tube's surface can increase operating temperature of the tube and decompose structural components.

Microstructure of tube wall material (16M steel) is shown at Fig. 3 and 4. Microstructure of both tube segments taken from the level 10 and 18 m from the bottom of combustion chamber show non degraded structure consisted of ferrite and bainite grains. The grain growth due to the high temperature operation was not detected.

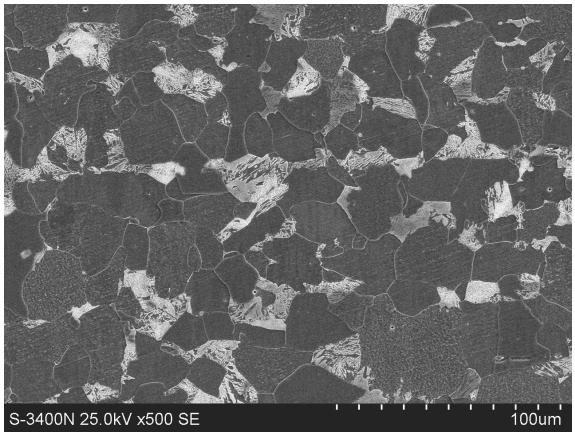

Fig. 3. Microstructure of 16M steel. Tube segment taken from the level of 10 m at combustion chamber, SEM image

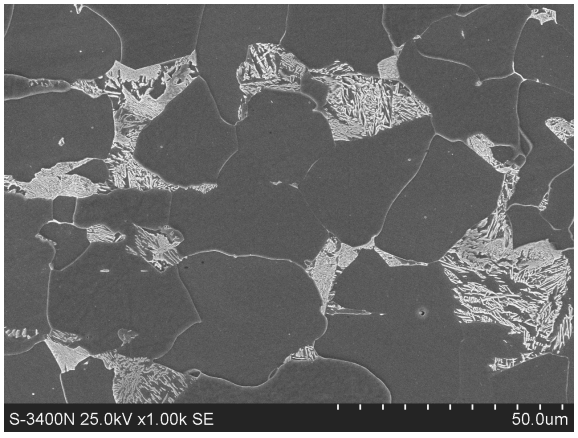

Fig. 4. Microstructure of 16M steel. Tube segment taken from the level of 18 m at combustion chamber, SEM image

Vickers hardness test has been performed according to standard PN-EN ISO 6507-1:2007. Results of hardness test are shown in Table 2. The differences in hardness on the cooler - insulation side and fire side of the tubes were not considerable. The hardness at fireside of the tube can decrease due to the bainite decomposition after long term exploitation, but in current investigations such effect has not been observed [10].

Table 2.
Results of Vickers hardness test

	Insulation side	Flu gases side
42D/10	170	163
42G/18	168	164
51D/10	169	161
51G/18	170	168

Tensile tests were performed on the samples taken from the fireside of the tubes in the form of 15 mm width segments. Tensile strength, proof strength and elongation were recorded and compared to the PN-85/H-74252 standard requirements for new material. Results of tests are shown in Table 3. Tube material after two years exploitation shows good mechanical properties. Only elongation seems to be unsatisfactory, but it is rather effect of pits on outer surface of the tube where stresses can concentrated and influence the flow of the material during the test.

Table 3.
Results of static tensile tests

Tube/ height from bottom, m	$R_{p0.2}$ MPa	R_m MPa	A_5 %
16M PN-85/H-74252	min 285	440-540	min 22
42D/10	405	504	18.9
42G/18	338	440	18.6
51D/10	375	498	21.2
51G/18	375	505	18.7

Samples with corrosion deposits were taken from each segment and immersed in Wood's alloy for metallographic examinations. The local microanalyses of chemical composition at selected points and linear distribution of elements on tube-wall cross sections were performed. Additionally dot maps for elements like sulfur, calcium, potassium and chlorine were analyzed. Examinations were conducted with the use of Philips XL30 scanning microscope equipped with EDS analyzer. Examples of local chemical composition microanalysis performed on the sample taken from level of 10 and 18 m are presented in Figs. 5-8 and Tables 4, 5.

Scales consist mainly of iron oxides with considerable amount of sulfides. Detected elements were not uniformly spaced at the scale. The bands reach in sulfur were detected as well as zones enriched in chlorine. More alkaline metals were observed at scales covered samples taken from the level of 18m. Maximum sulfur contents were 32% and chlorine about 6%.

Linear distribution of elements (Figs. 9 and 10) has shown the increased concentration of chlorine and alkaline metals in the areas adjacent to the interface of base material and scale. Such shape of element distribution is dominant for samples taken from the level of 18 m.

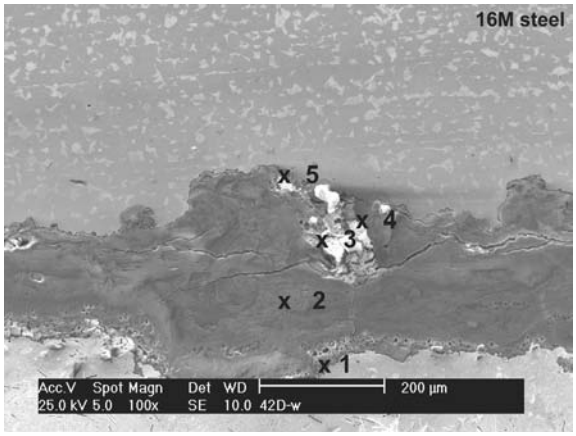

Fig. 5. Cross section of the fire side face of water wall tube. Sample 42D taken from the level of 10 m, "X" indicate points of spot analysis

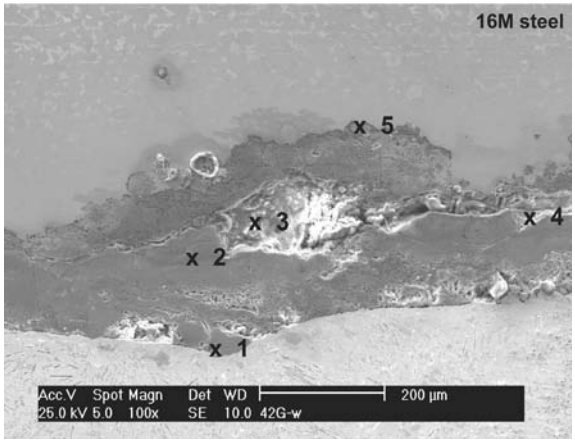

Fig. 6. Cross section of the fire side face of water wall tube. Sample 42G taken from the level of 18 m, "X" indicate points of spot analysis

Table 4.
Chemical analysis at the points indicated in Fig. 5 and 6 (wt. %)

	Na	Al	Si	S	Cl	K	Ca	Mn	Fe
42D									
1	0.0	0.85	0.73	1.8	0.62	1.38	0.43	0.85	bal
2	0.00	0.81	1.11	2.06	0.85	1.21	0.33	1.19	bal
3	0.00	0.74	0.99	4.47	2.24	2.77	0.76	0.49	bal
4	0.00	1.15	0.98	27.3	2.41	2.15	2.27	1.52	bal
5	0.00	1.09	1.44	11.9	1.57	0.76	1.81	1.55	bal
42G									
1	0.52	0.68	0.83	1.66	0.47	1.58	0.34	0.70	bal
2	0.93	0.00	0.62	1.33	0.31	1.42	0.37	0.71	bal
3	0.45	0.44	1.35	5.58	1.57	3.82	1.86	0.74	bal
4	1.34	0.00	1.01	4.15	1.53	5.60	1.93	1.45	bal
5	1.75	0.16	0.88	2.44	0.48	2.40	0.32	1.03	bal

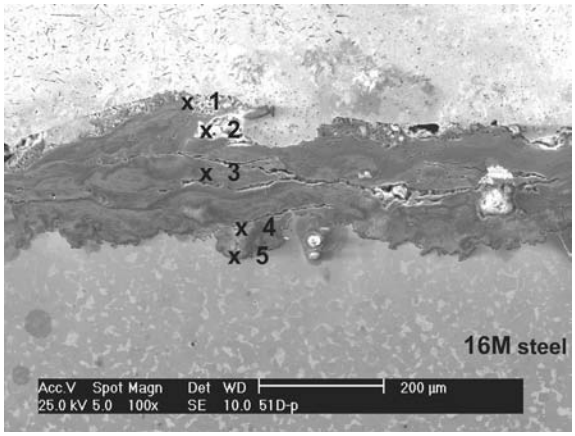

Fig. 7. Cross section of the fire side face of water wall tube. Sample 51D taken from the level of 10 m, "X" indicate points of spot analysis

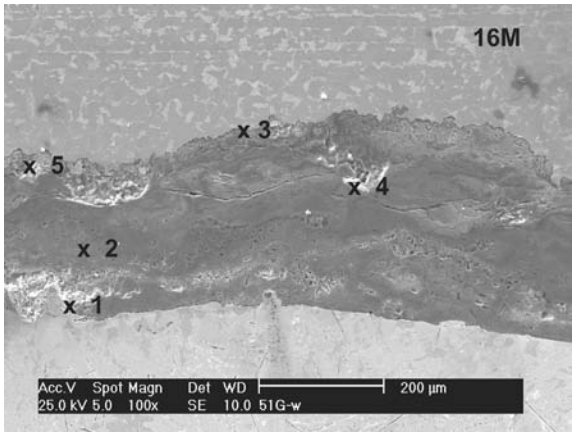

Fig. 8. Cross section of the fire side face of water wall tube. Sample 51G taken from the level of 18 m, "X" indicate points of spot analysis

Table 5.
Chemical analysis at the points indicated in Fig. 7 and 8 (wt. %)

	Na	Al	Si	S	Cl	K	Ca	Mn	Fe
51D									
1	0.00	0.29	0.35	1.13	0.77	0.68	0.38	0.74	bal
2	0.00	0.00	0.27	32.1	0.61	2.87	4.3	2.4	bal
3	0.00	0.00	0.58	1.63	0.75	1.12	0.40	0.65	bal
4	0.69	0.60	1.93	1.97	0.85	1.33	0.85	0.90	bal
5	0.75	0.93	1.37	1.68	0.85	3.13	1.03	1.11	bal
51G									
1	0.00	0.00	1.44	15.1	5.1	1.04	0.92	1.44	bal
2	0.55	0.63	0.80	1.16	1.44	5.56	0.76	0.93	bal
3	2.01	1.07	1.58	3.33	0.53	3.72	1.42	0.72	bal
4	1.05	2.27	3.81	6.45	1.35	2.99	1.29	0.78	bal
5	11.5	2.18	2.74	6.09	6.28	1.22	2.35	1.19	bal

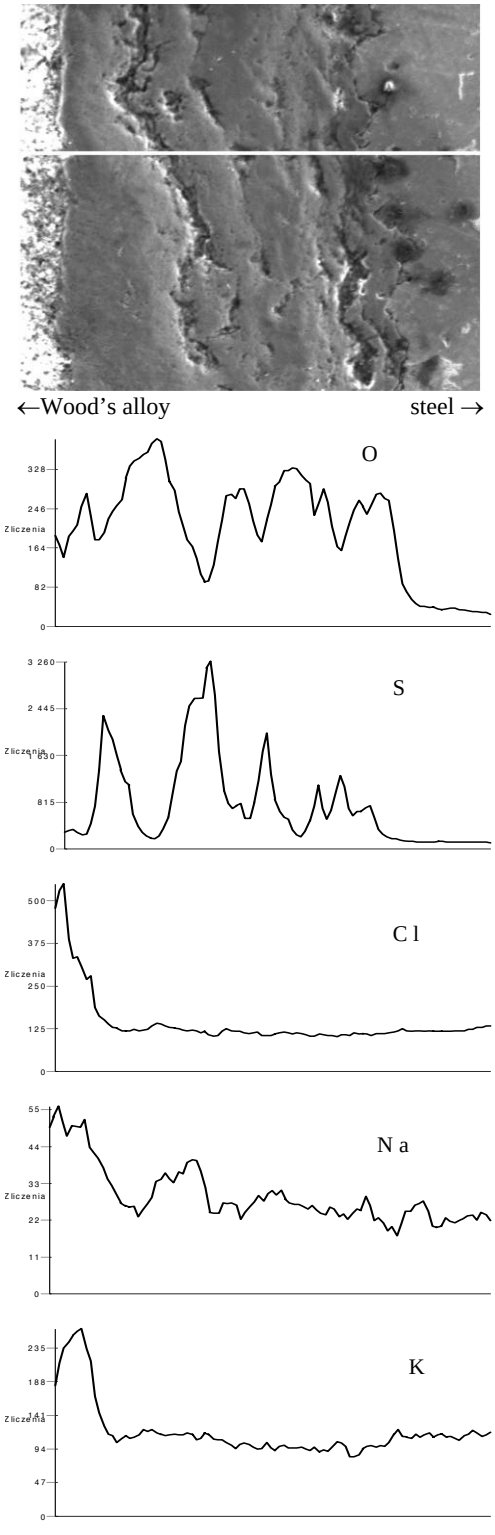

Fig. 9. Linear distribution of elements on cross section of deposit layer on ∅ 57 x 5.0 mm evaporator tube, level of 10 m

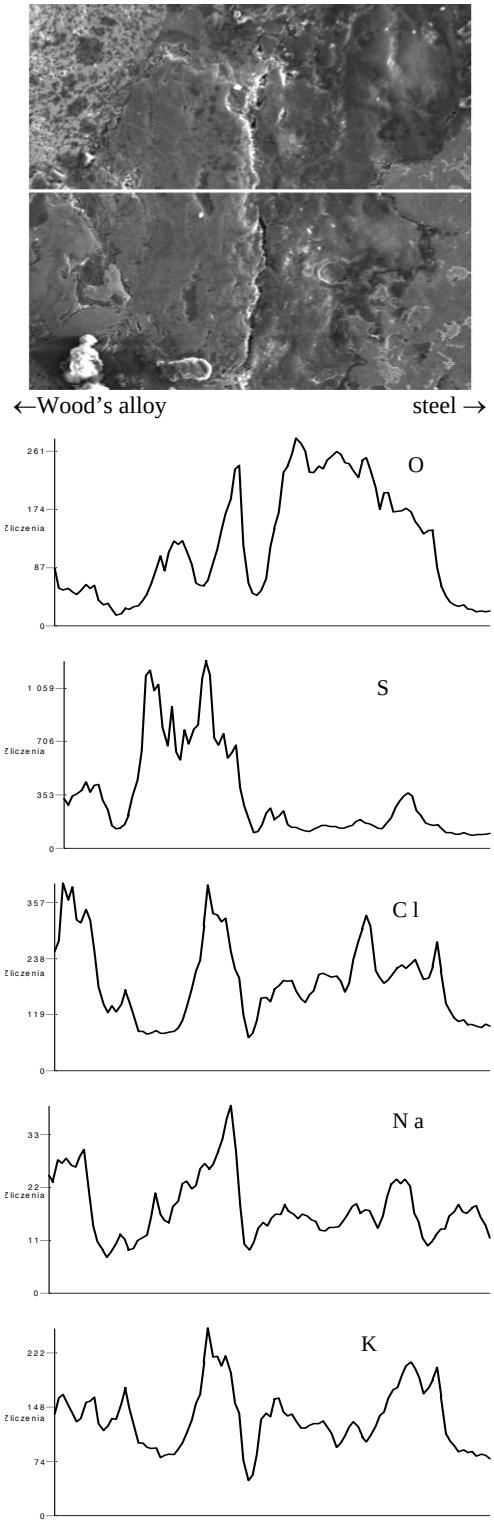

Fig. 10. Linear distribution of elements on cross section of deposit layer on ∅ 57 x 5.0 mm evaporator tube, level of 18 m

a)

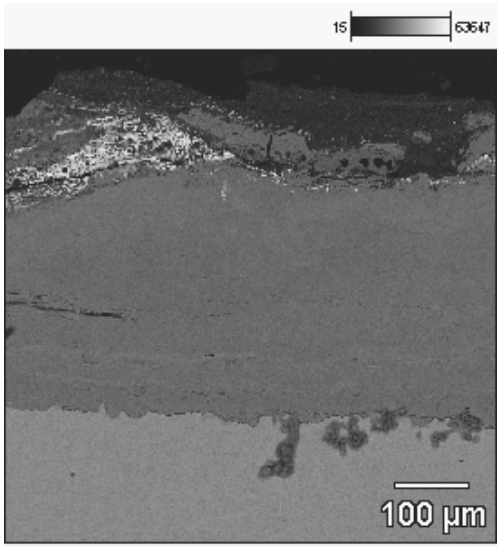

b)

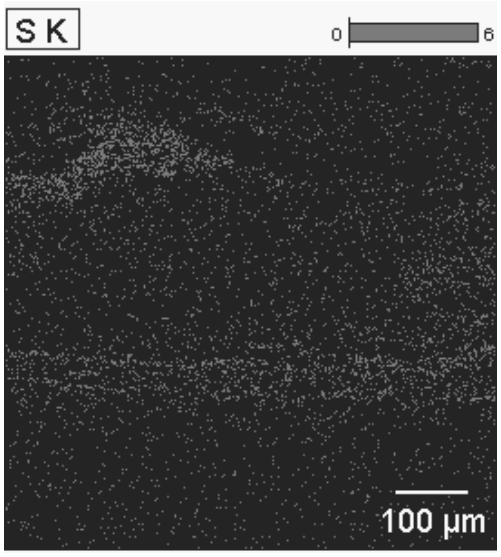

Fig. 11. Cross section of fire-side face of water wall tube subjected to reducing combustion conditions a) optical micrograph b) x-ray elemental dot map for sulphur

Dot maps confirmed observation on inhomogeneous of scale composition. Fig. 11 shows bands enriched in sulfur situated at external layer of the scale and second band close to the interface of base material and scale.

Detailed observations revealed pits and deep penetrations into the tube wall on the samples taken from the level of 18 m (Fig. 12). Such deep pits can form as a result of low melting ash constituent action. Local microanalyses of chemical composition (Figs. 13 and 14) indicated enriched concentrations of sulfur, chlorine and potassium close to the borderline of base material and scale.

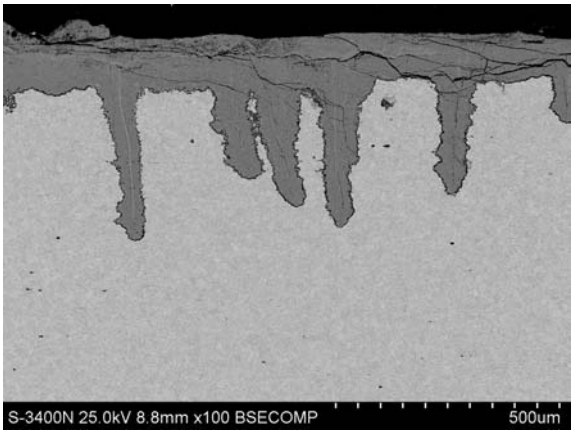

Fig. 12. Cross section of fire-side face of water wall tube, level - 18m. Dip penetrations into the tube wall

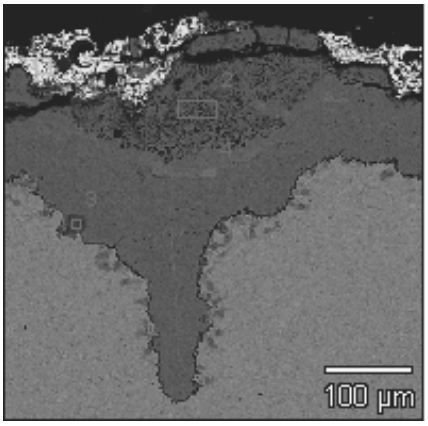

	Al	Si	S	Cl	K	Fe
1	3.36	6.72	11.41			bal
2	7.05	10.9	0.95		0.87	bal
3	0.58			2.46	1.14	bal
4		0.49	18.04			bal

Fig. 13. Chemical analysis of the scale at the corrosion pit (wt.%). Level - 18m, measure points indicated in micrograph

The chemical compounds existed in deposited layer was evaluated with the use of X-ray diffraction analysis. Deposits were scratched from the tube surface, then grinded and pressed. The quantitative chemical analysis of ions occurred in deposited layers was evaluated with the use of fluorescent X-ray and visible radiation spectroscopy on PLANITEST equipment. Results of the examinations are shown in Table 6.

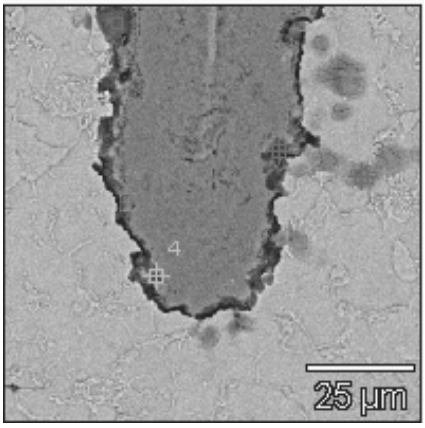

	Al	Si	S	Cl	K	Fe
1		1.47	0.62	0.73	0.82	bal
2		0.80	0.94	0.98		bal
3	0.43	0.44			1.01	bal
4		0.98	1.1	0.91		bal

Fig. 14. Chemical analysis of the scale at the tip of corrosion pit (wt. %). Level - 18m, measure points indicated in micrograph

Table 6.
Quantitative chemical analysis of ions in corrosion deposits

Deposits from level, m →	10	18
	Ion concentration, wt %	
Na^+	0.07	0.18
K^+	0.06	0.45
Mg^{2+}	0.06	0.18
Ca^{2+}	0.42	0.75
SO_4^{2-}	0.77	3.48
Cl^-	traces	0.12
CO_3^{2-}	0.38	0.63

Examinations show presence of the following compounds:
- iron oxides (Fe_3O_4, Fe_2O_3 and FeO) with dominant Fe_3O_4,
- iron sulfides (FeS, FeS_2),
- small amounts of sodium (Na) and potassium (K).

3. Discussion

Corrosion of the water wall tubes in low-emission steam boilers may be a result of reaction of steel tube surface with the aggressive substoichiometric environment contains sulfur. In oxidizing atmospheres sulfur reacts with oxygen to form SO_2 and SO_3. These oxygen-rich atmospheres are often much less corrosive than reducing atmospheres, where the sulfur is found in the form of H_2S. In reducing conditions iron sulfide is the expected corrosion product on iron rather than the iron oxides (Fe_3O_4, Fe_2O_3). That sulfide scales allow higher rates of transport of iron cations than oxides do, so they are less protective [1,3,11]. Reducing conditions can also lower melting temperature of any deposited slag. It leads to local disruption of the oxide film on the wall tubes and accelerated oxidation or to oxidation-sulfidation. In coal fired boilers, alkali sulfates deposited on the water walls may react with SO_2 and SO_3 to form pyrosulfates which have melting points of 330 to 410°C. The role of chlorine is not well known so far. The presence of this element in reducing combustion atmosphere is reported to enhance corrosion rate. Chlorine probably reacts with oxide scales making them brittle and causing blistering and cracking. Coal with more than about 0.2% Cl may result in accelerated fireside corrosion for furnace water walls under reducing conditions [1].

Examination results of the ∅ 57 x 5.0 mm water wall tube show that both mechanisms of corrosion (sulfide and molten salts) took place. Chemical analysis indicated presence of alkaline metals (K, Na, Mg, Ca) and iron sulfides (FeS, FeS_2) in the scale. The morphology of scales consisted of two layers. External, this is porous and weakly connected with the tube surface, and internal, which is dense and adherent to the base metal. In these two layers the bands reach in sulfur were detected. Concentration of S in such bands reached 32 wt. %.

Considering the tubes wall thickness it is visible that the less reduction of thickness occurred on the level of 18 m. X-ray chemical analysis did not indicate large differences in sulfur contents in tubes on tested levels 10 and 18 m, but differences in ion concentrations (SO_4^{2-}, Cl^-, Na^+, K^+) were considerable, higher on the level 18 m in comparison to lower one. Concentrations of such elements like S, Cl, K, were higher in vicinity of borderline scale and base metal area. Detailed microscopic examinations of this zone revealed deep corrosion pits (Fig. 13). Such corrosion mechanism is typical when molten salt appear on tube surface. This indicates that molten salt corrosion is dominating in higher levels in combustion chamber. Limitation of effects of sulfide corrosion can be attributed to lower temperature in this zone and to influence of secondly air from over fire air (OFA) nozzles.

The corrosion intensity on the lower level of 10 m is mainly due to sulfide corrosion. Smaller amounts of SO_4^{2-} and alkaline metals indicate that progress of salt corrosion is limited (comp.: [12, 13, 14, 15]).

It is worth to indicate that only traces of chlorine was detected in the scale on the level of 10 m, but on 18 m Cl^- concentration was considerably higher.

4. Conclusions

- Substoichiometric combustion conditions in low NO_x emission boiler caused sulfide corrosion and molten salt corrosion of water wall tubes surfaces.
- Tube's wall thickness reductions reach 58% of its nominal value after two years of exploitation.

- The wall thickness examinations of evaporator tubes indicated that reduction of thickness was considerable on the segments taken from level of 10m, when at level of 18 m this reduction was smaller.
- The morphology of scales consisted of external, porous and weakly connected layer and internal, which was dense and adherent to the base metal. In that two layers the bands reach in sulfur were detected.
- The sulfide corrosion seems to be the main degradation mechanism of water wall tubes in combustion chamber at the level of 10 m where reducing conditions occur.
- The molten salt corrosion dominates on higher levels of combustion chamber.

References

[1] G. Y. Lai, High-temperature corrosion of engineering alloys, ASM Internationa, 1997, 1.
[2] Metals Handbook, Failure Analysis and Prevention. ASM International, 1995, 11.
[3] Metals Handbook, Corrosion, ASM International, 1987, 13.
[4] Hernas, Creep resistance of steel and alloys. Silesian University of Technology, Gliwice, 1999 (in Polish).
[5] J. Łabanowski, Mechanical properties and corrosion resistance of dissimilar stainless steel welds, Archives of Materials Science and Engineering 28/1 (2007) 27-33.
[6] J. Nowacki, P. Rybicki, Corrision resistance of SAW duplex joints welded with high heat input, Journal of Achievements in Materials and Manufacturing Engineering 23/2 (2007) 7-14.
[7] J. Łabanowski, S. Topolska, J. Ćwiek, Assessment of evaporator tubes corrosion in low-emission steam boilers, Advances in Materials Science 8/4 (2008) 14-21.
[8] S. Król, M. Pietrzyk, Formation of corrosion products protecting surfaces of the boiler proper tubes from the combustion chamber, Journal of Achievements in Materials and Manufacturing Engineering 21/2 (2007) 45-48.
[9] J. Okrajni, K. Mutwil, M. Cieśla, Steam pipelines effort and durability, Journal of Achievements in Materials and Manufacturing Engineering 22/2 (2007) 63-66.
[10] J. Pacyna, The microstructure and properties of the new bainitic rail steels, Journal of Achievements in Materials and Manufacturing Engineering 28/1 (2008) 19-22.
[11] S. Mrowec, T. Weber, The modern heat resistant materials, WNT, Warsaw, 1982 (in Polish).
[12] A. Zieliński, J. Dobrzański, G. Golański, Estimation of the residual life of L17HMF cast steel elements after long-term service, Journal of Achievements in Materials and Manufacturing Engineering 34/2 (2009) 137-144.
[13] J. Nowacki, P. Zając, Microstructure and corrosion resistance of the duplex steel wide-gap one-side fluxcored wire welded joints, Journal of Achievements in Materials and Manufacturing Engineering 28/2 (2008) 191-198.
[14] D. Renowicz, A. Hernas, M. Cieśla, K. Mutwil, Degradation of the cast steel parts working in power plant pipelines, Journal of Achievements in Materials and Manufacturing Engineering 18/1/2 (2006) 219-222.
[15] J. Okrajni, Thermo-mechanical fatigue conditions of power plant components, Journal of Achievements in Materials and Manufacturing Engineering 33/1 (2009) 53-61.